

Stereoselective interactions of lactic acid enantiomers with HSA: Spectroscopy and docking application

Hongtao Mu^a, Shaohuan Chen^a, Fengyin Liu^a, Jianbo Xiao^b, Hui Huang^c, Yuhua Zhang^a, Yuanming Sun^d, Xiangyang Gao^e, Hongtao Lei^{d,*}, Xuewen Yuan^{a,*}

^a College of Biology and Food Engineering, Guangdong University of Education, Guangzhou 510303, China

^b Institute of Chinese Medical Sciences, State Key Laboratory of Quality Research in Chinese Medicine, University of Macau Taipa, Macau

^c South China Sea Fisheries Research Institute, Chinese Academy of Fishery Sciences, Guangzhou 510300, China

^d Guangdong Provincial Key Laboratory of Food Quality and Safety, South China Agricultural University, Guangdong Provincial Engineering & Technique Research Centre of Food Safety Detection and Risk Assessment, Guangzhou 510642, China

^e College of Food Science, South China Agricultural University, Guangzhou 510642, China

ARTICLE INFO

Keywords:

Lactic acid isomers
Human serum albumin
Fluorescence spectroscopy
Circular dichroism
Docking simulation

ABSTRACT

Lactic acid enantiomers, normally found in fermented food, are absorbed into the blood and interact with plasma carrier protein human serum albumin (HSA). Unveiling the effect on the function and structure of HSA during chiral interaction can give a better understanding of the different distribution activities of the two enantiomers. Multi-spectroscopic methods and molecular modelling techniques are used to study the interactions between lactic acid enantiomers and HSA. Time-resolved and steady-state fluorescence spectra manifest that the fluorescence quenching mechanism is mainly static in type, due to complex formation. Binding interactions, deduced by thermodynamic calculation, agree with the docking prediction. Docking results and kinetic constants represent chiral-recognizing discriminations consistently. The bindings of lactic acid enantiomers lead to some microenvironmental and slight conformational changes of HSA as shown by circular dichroism (CD), synchronous and three-dimensional fluorescence spectra. This investigation may yield useful information about the possible toxicity risk of lactic acid enantiomers to human health.

1. Introduction

Lactic acid affects the rheological and sensory qualities of milk and gives good storage properties to fermented products. As a nutrient, it provides 3.6 kcal/g or 15.2 kJ/g of energy (Alm, 1982). Lactic acid is chiral, consisting of two optical enantiomers (Fig. 1). One is L-(+)-lactic acid (L-Lac) and the other is D-(-)-lactic acid (D-Lac). Lactic acid enantiomers are characteristic in all fermented dairy products (wines, sake and milk products) which are generated by both homo- and heterofermentative microbes. In fermented milk (Alm, 1982), the amount of total lactic acid is about 0.6–1.2%, and L-Lac is the major enantiomer formed. The amount of D-Lac is about 0–10% of the total lactic acid in acidophilus milk. In yogurt, about 40% of the total lactic acid is D-enantiomer.

Physiological experiments in man and animals showed that lactic acid enantiomers were absorbed from the human intestinal tract (Duran, Van Biervliet, Kamerling, & Wadman, 1977). L-Lac can promote calcic absorption. However, the rate of metabolism of the D-enantiomer

was considerably lower than that of L-Lac (Flemström, 1971). However, after intake of large quantities of D-Lac, enhanced Ca²⁺ was secreted in the urine (Alm, 1982). Restricted consumption of products which contain a high concentration of D-Lac is worth advocating. Infant formulae containing D- or DL mixture should be avoided (Organization, 1974).

It is known that ligand–protein interactions affect the distribution, free concentration, and metabolism of various small molecules in the bloodstream. When lactic acid enantiomers are absorbed into the blood, they may bind to plasma proteins and subsequently change the structure and function of the protein. Yet, no reports have so far examined the chiral effects of lactic acid enantiomers at the molecular level, and the possible effect on plasma proteins is still poorly understood. Nutrition and safety of foods are concerns around the world, and thus information is needed to fill in this gap.

HSA is the major protein component of human blood plasma. The physiological and pharmacological functions of HSA are maintaining osmotic pressure of blood, buffering pH, and serving in the

* Corresponding authors.

E-mail addresses: hongtao@scau.edu.cn (H. Lei), yuanxuewen@gdei.edu.cn (X. Yuan).

<https://doi.org/10.1016/j.foodchem.2018.07.135>

Received 7 February 2018; Received in revised form 2 July 2018; Accepted 19 July 2018

Available online 20 July 2018

0308-8146/© 2018 Published by Elsevier Ltd.

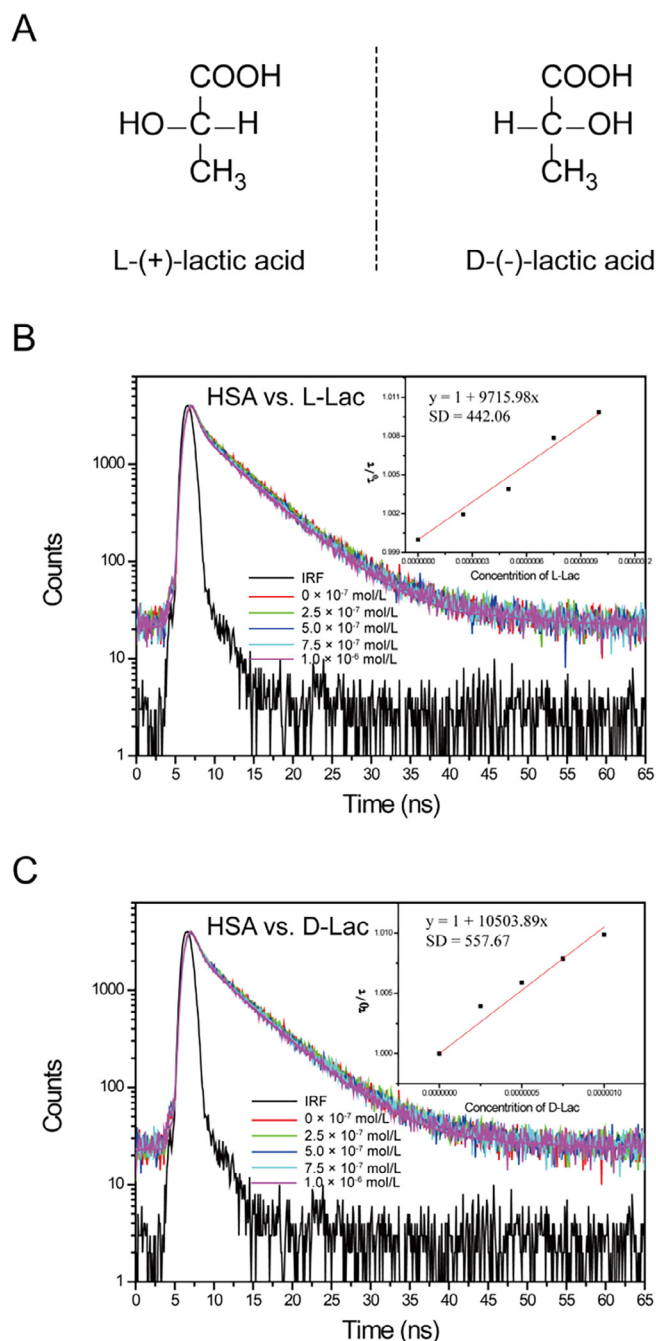


Fig. 1. (A) Structures of lactic acid isomers and fluorescence intensity decay of HSA (1.0×10^{-6} M) in presence of increasing (B) L-Lac and (C) D-Lac. Inset: dynamic SV constant K_{SV} regression. IRF: instrument response function.

transportation and distribution of a variety of nutrients and medicines. HSA is a monomeric protein which contains 585 residues. It contains 3 structurally similar α -helical domains (I–III), and each domain can be divided into subdomains A (containing 6 α -helices) and B (containing 4 α -helices) (He & Carter, 1992). Drugs or compounds mainly bind to one of the two primary binding sites on the protein, known as Sudlow's sites I (warfarin binding site) and II (benzodiazepine binding site).

Exploring the interaction mechanism of lactic acid enantiomers with HSA can give a better understanding of the different distribution activities of the two enantiomers. Because of their high sensitivity, rapidity, reproducibility, and convenience, spectroscopic approaches have become useful techniques for study of protein–ligand interactions (Cao et al., 2018; Zhang, Wang, & Pan, 2012). The measurements can

be carried out under physiological conditions to better mimic *in vivo* interaction environments (Mu et al., 2018; Zhang, Zhuang, Tong, & Liu, 2013). Multi-spectroscopic approaches, such as time-resolved fluorescence, steady-state fluorescence quenching, three-dimensional (3D) fluorescence, synchronous fluorescence and CD spectroscopy, were used to determine the binding characteristics, the main acting forces and conformational changes during chiral binding. The molecular docking technique was also employed to further elucidate chiral binding. This method is easily applicable to find out the preferred orientation of one or more molecules on the active sites of proteins (Liu et al., 2018). In the meantime, the binding affinity may be predicted, using the preferred orientation. Molecular docking has been successfully employed to further elucidate the mechanism of chiral binding, because it has the ability to predict the optimal conformations between small molecules and the binding sites of protein (Alonso, Bliznyuk, & Gready, 2006). Spectra and docking results may provide basic data for clarifying the stereoselective binding mechanisms of L-Lac/D-Lac with HSA and may be helpful for human health and food safety.

2. Materials and methods

2.1. Materials

L-(+)-Lactic acid (90% in water) and D-(-)-lactic acid (89–91%) were purchased from Adamas Reagent, Ltd. (Shanghai, China). HSA (96–99%) was obtained from Sigma-Solarbio Co. (Beijing, China). Other reagents and chemicals used in this research were all of analytical grade or higher level. Deionized water (18.2 M Ω) was prepared using a Milli-Q water purification system (Millipore, Bedford, MA). Tris–HCl buffer solution (0.1 M NaCl, 0.1 M Tris, pH 7.40) was used in fluorescence measurement, and phosphate buffer (0.02 M, pH 7.40) was used in circular dichroism measurements.

2.2. Steady-state fluorescence measurements

Steady-state fluorescence spectra measurements were performed on a Cary Eclipse Spectrofluorimeter (Varian, USA) equipped with CARY Temperature Controller (–10–110 °C). Excitation wavelength of 280 nm was used for fluorescence emission spectra measurement. Fluorescence titrations were performed by keeping the fixed concentration of HSA (4.30×10^{-7} M) while titrating by successive additions of L-Lac or D-Lac at temperatures of 293 K, 301 K and 310 K. The lactic acid concentrations after each titration were 1.28, 2.56, 3.84, 5.12, 6.40, 7.68, 8.96, 10.2, 11.5×10^{-7} M, respectively. The synchronous fluorescence spectra were obtained by setting the excitation and emission wavelength interval ($\Delta\lambda$) at 15 and 60 nm (298 K). The 3D fluorescence spectra of L, D-Lac (1.15×10^{-6} M), HSA (4.30×10^{-7} M) and mixtures of HSA-Lac enantiomer were obtained in an excitation wavelength range from 200 nm to 320 nm at 5 nm increments at temperature of 298 K, and emission wavelength range from 280 nm to 480 nm and recorded.

2.3. Time-resolved fluorescence experiments

A FLS980 system (Edinburgh Instruments) equipped with a 290.80 nm picosecond pulsed light emitting diode was used for time-resolved fluorescence decays measurement. The emission monochromator was fitted to 346 nm with slits of 10 nm. The fluorescence decay curves were recorded over 100 ns up to a peak count of 4000 (1024 channels) at 301 K. The decay curves of HSA (1.0×10^{-6} M) were measured with 0, 2.5, 5.0, 7.5, 10×10^{-7} M lactic acid isomers. The intensity decays were fitted using the FAST software package (Edinburgh Instruments).

2.4. CD studies

A Jasco J-810CD spectrometer (Japan Spectroscopic, Japan) with a 0.1 cm quartz cell was used for CD spectra measurement. Phosphate buffer solution (0.02 M, pH 7.40) was used to avoid the influence of chloride ions. The spectra of HSA (1.5×10^{-6} M) and HSA mixed with 1.5×10^{-6} M lactic acid enantiomer were measured in the range of 190–250 nm with a scan rate of 100 nm/min. Each spectrum was accumulated by taking an average of three separate scans. Secondary structure of protein was analyzed by Jasco SSE (Secondary Structure Estimation) software.

2.5. Molecular docking study

The crystal structure of HSA in complex with *R*-warfarin (PDB ID: 1H9Z) was downloaded from Brookhaven Protein Data Bank and was chosen as the docking template. The 3D structures of *L*-, and *D*-lactic acid were constructed and minimized using UCSF Chimera (Pettersen et al., 2004). AMBER ff14SB force field and AM1-BCC charges were assigned for both HSA and ligands (Jakalian, Bush, Jack, & Bayly, 2000; Jakalian, Jack, & Bayly, 2002). Lactic acid analogue stereoisomers were docked into the HSA spheres, using the standard flexible-ligand sampling algorithm (Mukherjee, Balius, & Rizzo, 2010) implemented in DOCK 6.7 (Allen et al., 2015). The maximum number of orientations was increased to 10000. In order to select energetically favourable docking positions for each ligand, the combined grid Van-der-Waals and electrostatic (vdw + es) scores and internal energy scores for poses was performed. The top scoring poses were visualized using PyMOL (Schrödinger, 2015).

3. Results and discussion

3.1. The effect of H^+ on emission fluorescence spectra

Lactic acid is an organic compound, and is classified as an α -hydroxy acid. Lactic acid in solutions can release H^+ , and the solutions become acidic. Can the H^+ released by lactic acid affect the quenching spectrum between lactic acid enantiomers and HSA? To clarify this question, we titrated increased amounts of HCl into HSA solution. The result (Fig. S1) showed that the additional H^+ (up to 11.5×10^{-7} M) did not affect the fluorescence quenching between lactic acid enantiomers and HSA. Tris-HCl buffer solution (0.1 M, pH 7.40) played a key role in stabilizing the acid-base environment.

3.2. Fluorescence quenching between HSA and lactic acid enantiomers

To gain deeper insight into the underlying quenching processes, both time-resolved and steady state fluorescence were used in this study. The quenching of the intrinsic fluorescence of HSA by lactic acid enantiomers may be caused by inter- or intra-molecular processes such as complex formation (static quenching), molecular collisions (dynamic quenching), energy transfer and conformational changes, or a combined mechanism (Ali & Al-Lohedan, 2018; Siddiqui, Siddiqi, Khan, & Naem, 2018).

Life-time measurements are unequivocally employed to explore dynamic or static quenching mechanisms (Ghosh, Rath, & Arora, 2016; Lakowicz, 2013). Fig. 1 shows the fluorescence decay curves of HSA in the absence and presence of lactic acid enantiomers. The decay curves were fitted as biexponential functions achieving the optimal fitting residuals and acceptable χ^2 values. Fluorescence decay fitting parameters and the average fluorescence lifetime of the lactic acid-HSA system are shown in Table S1. The dynamic SV constant K_{SV} can be obtained as.

$$\tau_0/\tau = 1 + K_{SV}[Q] \quad (1)$$

where τ_0 and τ denote average lifetimes of HSA in the absence and

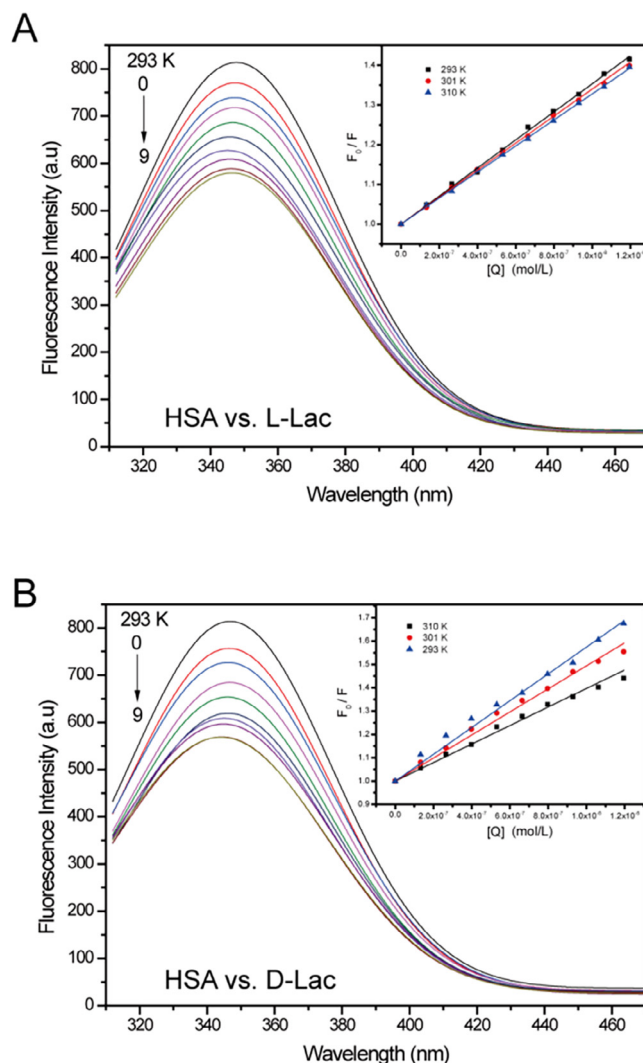


Fig. 2. Fluorescence spectrum of HSA (4.30×10^{-7} M) in presence of increasing amounts of (A) *L*-Lac and (B) *D*-Lac 1.28×10^{-7} M per micro-titration. Inset: Stern–Volmer plots at three temperatures.

presence of lactic acid enantiomers, respectively; K_{SV} means dynamic Stern–Volmer constant, and $[Q]$ represents the concentration of lactic acid enantiomers. Based on Eq. (1), dynamic SV constants, K_{SV} , were determined as 1.05×10^4 L/mol (Adj. $R^2 = 0.999$) for *D*-Lac and 9.72×10^3 L/mol (Adj. $R^2 = 0.999$) for *L*-Lac (Fig. 1 inset).

The steady-state fluorescence can reveal both dynamic and static quenching, based on grounds of temperature-dependence of the respective quenching constants. Static quenching is recognized to form a complex substance; if temperature increases, the static quenching constant will decrease, while a higher temperature will disturb the stability of the complex (Zhang & Ni, 2017). But the opposite effect will be deemed as dynamic quenching (Tang, Li, Bi, & Gao, 2016). Figs. 2 and S2 show the fluorescence emission spectra of HSA with the addition of lactic acid enantiomers. The peak at 348 nm is deemed as the characteristic fluorescence emission of HSA, which is mainly contributed by tryptophan (Trp) residues (Shen, Gu, Jian, & Qi, 2013). The steady-state Stern–Volmer equation was used for data processing.

$$F_0/F = 1 + K_{SV}[Q] = 1 + k_q\tau_0[Q] \quad (2)$$

where F_0 and F represent fluorescence intensities of the HSA in the absence and presence of lactic acid enantiomers, respectively; K_{SV} means the Stern–Volmer quenching constant; $[Q]$ represents the molar concentration of lactic acid enantiomers; k_q denotes the quenching rate

Table 1

Binding constants (K_a), and number of binding sites (n) and relative thermodynamic parameters of HSA and lactic acid isomers at temperatures of 293 K, 301 K, and 310 K. (pH = 7.4).

Interaction system	T (K)	$K_{SV}10^3$ (l/mol)	$K_{SV}10^5$ (l/mol)	$k_q 10^{13}$ (l/(mol·s))	$K_a 10^5$ (l/mol)	n	$\Delta H^\circ 10^4$ (kJ/mol)	$\Delta G^\circ 10^4$ (kJ/mol)	ΔS° (J/(mol·K))
HSA vs. L-Lac	293	–	3.54	3.54	2.64	0.979	–4.41	–3.04	–46.8
	301	10.5	3.30	3.30	2.39	0.975		–3.10	–43.6
	310	–	3.29	3.29	0.985	0.912		–2.96	–46.8
HSA vs. D-Lac	293	–	5.74	5.74	1.40	0.925	–6.40	–2.89	–120
	301	9.72	4.94	4.94	1.14	0.894		–2.91	–116
	310	–	3.91	3.91	0.334	0.797		–2.69	–120

constant of HSA; τ_0 means the average lifetime of the free HSA molecule, and its value is 5.12 ns (Table S1). K_{SV} was determined by linear regression of a plot of F_0/F vs. $[Q]$.

As shown in the results (Table 1 and Fig. 2 (inset)) the K_{SV} values (10^5 L/mol, 301 K) obtained from fluorescence quenching measurement are ten-fold larger than those (K_{SV} , 10^3 L/mol) measured by time-resolved fluorescence (Table 1). Besides, the K_{SV} of the HSA with lactic acid enantiomers has an opposite trend as the temperature increases and the values of k_q (10^{13} L/(mol·s)) are much greater than the limiting diffusion rate constant of the biomacromolecule (2.0×10^{10} L/(mol·s)). The evidence indicates that the quenching was mainly initiated by static quenching (Matei, Ionescu, & Hillebrand, 2011; Shiri, Rahimi-Nasrabadi, Ahmadi, & Ehrlich, 2018). That is to say, the ground-state complex was formed during the process of lactic acid enantiomers binding to HSA.

3.3. Chiral binding constant and the number of binding sites

Generally, the binding constant (K_a) and number of binding sites (n) in a static-quenching process can be determined by plotting the double logarithm regression curve of the fluorescence data with another modified Stern–Volmer equation (Tang, Huang, et al., 2016).

$$\lg(F_0 - F)/F = \lg K_a + n \lg[Q] \quad (3)$$

K_a , as a special case of the kinetic equilibrium constant, is associated with the binding and unbinding processes between protein and ligands. The K_a of HSA with the L-Lac system was twofold larger than that of HSA with the D-Lac system (Table 1), indicating that the binding affinity of L-Lac was stronger than that of D-Lac. Results also showed that the values of K_a decreased with increasing temperature, implying that the complex of lactic acid enantiomers with HSA becomes unstable with the rising temperature. As shown in Table 1, The values of n are approximately equal to 1, which indicates that about one binding site on the HSA was combined while the binding reaction reached its balance.

3.4. Interaction force type prediction

The main non-covalent forces promoting interactions between proteins and ligands can be attributed to van der Waals forces, hydrogen bonds, and electrostatic and hydrophobic interactions. The driving forces of the binding reaction can be determined by thermodynamic parameters. Those parameters include Gibbs free energy change (ΔG°), entropy change (ΔS°) and enthalpy change (ΔH°). The values of these parameters in the lactic acid–HSA binding process can be calculated according to the Van't Hoff equation (Tang, Li, et al., 2016; Tang, Huang, et al., 2016).

$$\ln(K_2/K_1) = \Delta H^\circ(1/T_1 - 1/T_2)/R \quad (4)$$

$$\Delta G^\circ = -R T \ln K_a \quad (5)$$

$$\Delta S^\circ = (\Delta H^\circ - \Delta G^\circ)/T \quad (6)$$

where T is the absolute temperature, K is the binding constant (K_a) at a certain temperature, R denotes the gas constant, and its value is 8.314 J/(mol·K). If the temperature does not vary significantly, the ΔH°

can be regarded as a constant. The specific interaction mode can be determined by the values of ΔH° and ΔS° as follows:

(1) if $\Delta H^\circ \approx 0$ and $\Delta S^\circ > 0$, then electrostatic forces predominate, (2) if $\Delta H^\circ < 0$ and $\Delta S^\circ < 0$, then van der Waals forces and hydrogen bonds predominate, (3) if $\Delta H^\circ > 0$ and $\Delta S^\circ > 0$, then hydrophobic forces predominate (Ross & Subramanian, 1981; Zhang et al., 2013).

The results calculated from Eqs. (4)–(6) are shown in Table 1. The negative values of ΔG° mean that the binding process is spontaneous at the corresponding temperature. For both chiral interacting models, ΔS° and ΔH° are all negative, which indicates that van der Waals forces and hydrogen bonds quite possibly play a leading role in the chiral binding. In addition, all interactions between HSA and lactic acid isomers were induced mainly by enthalpy because of the very small entropy change.

3.5. Analysis of micro-environment changes of tyrosine (Tyr) and tryptophan during chiral recognition, using synchronous fluorescence and three-dimensional fluorescence spectra

To study micro-environment changes of Tyr and tryptophan during chiral recognition, synchronous fluorescence and three-dimensional fluorescence methods were used. Spectroscopy of synchronous fluorescence is a practical method for studying the micro-environment changes near the chromophore residues because this method has good sensitivity, simplicity, avoidance of different perturbing effects, and bandwidth reduction (Wang, Zhang, & Wang, 2014). The characteristic information of the Trp and Tyr residues can be obtained when the wavelength intervals between the emission and excitation wave-length ($\Delta\lambda = \lambda_{em} - \lambda_{ex}$) are set at 15 and 60 nm, respectively (Cao et al., 2018; Congdon, Muth, & Splittgerber, 1993). The wavelength shift of the emission spectral peak (λ_{max}) of the molecule is related to the polarity around the chromophore residues (Gu, Wang, & Zhang, 2018; Yuan, Weljie, & Vogel, 1998). Fig. 3 shows the synchronous fluorescence spectra during chiral interaction. There was no obvious shift at $\Delta\lambda = 60$ nm for either L-Lac or D-Lac with the HSA interaction system. But, at $\Delta\lambda = 15$ nm, there was a slight blue shift (about 2 nm) for L-Lac vs. The HSA system and a small red shift (about 2 nm) for the D-Lac vs. HSA interaction system. The results denoted that the conformation of HSA was slightly perturbed during chiral interaction. The observed red shift for the HSA vs. D-Lac system indicated that the micro-environment of Tyr residues changed from a nonpolar hydrophobic state to a more hydrophilic one. The observed blue shift for the HSA vs. L-Lac system indicated that the micro-environment of Tyr residues changed to a more hydrophobic condition. The results show that the micro-environment of Tyr residues was changed and the conformations of HSA were also slightly changed during the chiral ligand binding.

The conformational changes of HSA were also investigated by the 3D fluorescence spectroscopy technique. The 3D fluorescence spectra changes of HSA in absence and presence of lactic acid enantiomers were compared and analyzed. There are two hump-like peaks in the 3D fluorescence spectra (Fig. S3). The peak *a* ($\lambda_{ex} = 220$ nm, $\lambda_{em} = 334$ nm) mainly resulted from the polypeptide backbone structures (peptide bonds). Peak *b* ($\lambda_{ex} = 280$ nm, $\lambda_{em} = 348$ nm) was primarily contributed by the characteristic spectra of Trp and Tyr residues. The fluorescence intensities of those two peaks decreased obviously

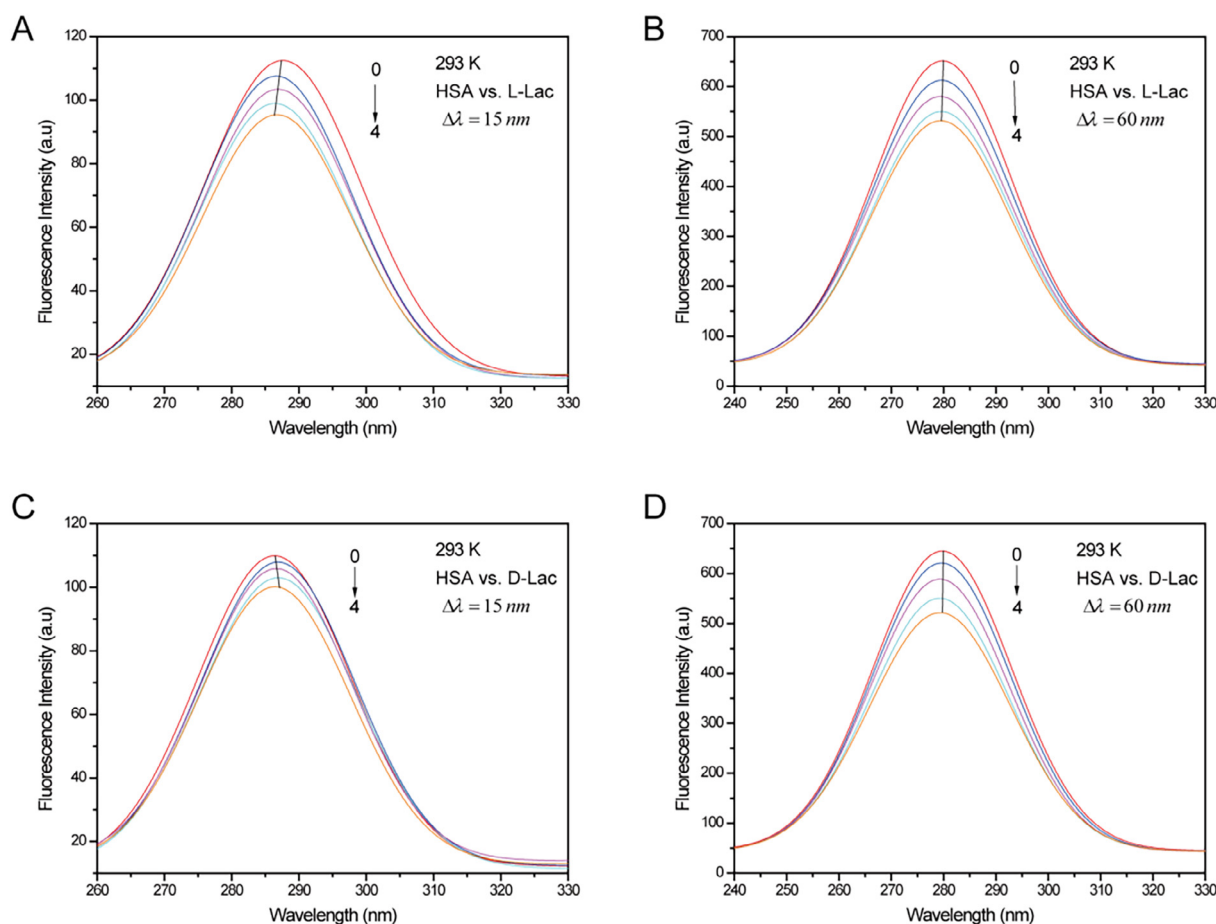


Fig. 3. Synchronous fluorescence spectra of HSA (4.30×10^{-7} M) in the absence (0) and presence (1–4) of increasing amounts (2.56×10^{-7} M per micro-titration) of (A and B) L-Lac and (C and D) D-Lac. T = 298 K.

when L-Lac or D-Lac was added, which indicates that the presence of L-Lac/D-Lac might induce slight unfolding of the HSA polypeptides. The results obtained from synchronous fluorescence and three-dimensional fluorescence spectra agree with each other.

3.6. The effect of chiral combination on HSA secondary structure changes

The secondary structure changes of HSA were studied using the CD technique. Fig. 4 shows the CD spectra of HSA in the absence and presence of lactic acid enantiomers under physiological conditions (pH = 7.4). The far ultraviolet CD spectra of HSA containing negative peaks at 209 and 222 nm reflects the characteristic α -helical structure assignable to $\pi \rightarrow \pi^*$ and $n \rightarrow \pi^*$ transfers, which are typical of the α -helical structure of any protein (Kelly, Jess, & Price, 2005). With the addition of chiral ligand, the secondary structures of HSA were slightly changed (Fig. 4 and Table S2). Based on the experimental dichroic spectra, the percentages of α -helix, β -sheet, β -turn and random coil conformations of HAS, in the absence and presence of lactic acid enantiomers, were computed using CDNN Circular Dichroism Spectroscopy software. The calculated results showed a decrease in the α -helix and β -sheet and an increase in the β -turn and random coil structures at a molar ratio of HSA to L-Lac/D-Lac of 1:1. The result revealed that α -helix and β -sheet were probably affected by the insertion of lactic acid into the hydrophilic pocket of HSA.

3.7. Docking analysis of chiral combination

Molecular docking was employed as a complementary way to help understand chiral ligands–HSA interaction. HSA has seven possible

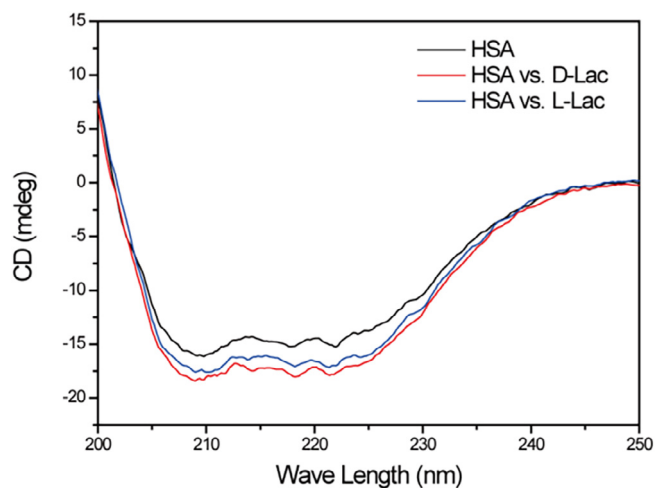


Fig. 4. Circular dichroism spectra of HSA (1.0×10^{-6} M) in the absence (black line) and presence of L-Lac (1.0×10^{-6} M, blue line) and D-Lac (1.0×10^{-6} M, red line). (For interpretation of the references to colour in this figure legend, the reader is referred to the web version of this article.)

binding sites for endogenous and exogenous ligands. To find the lactic acids' binding site, L-Lac/D-Lac enantiomers were docked into every putative binding site, and the optimal docking conformations in each putative binding site were obtained. Among the seven docking conformations, the pose which had the lowest score was chosen as the binding conformation and this binding site was recognized as the lactic

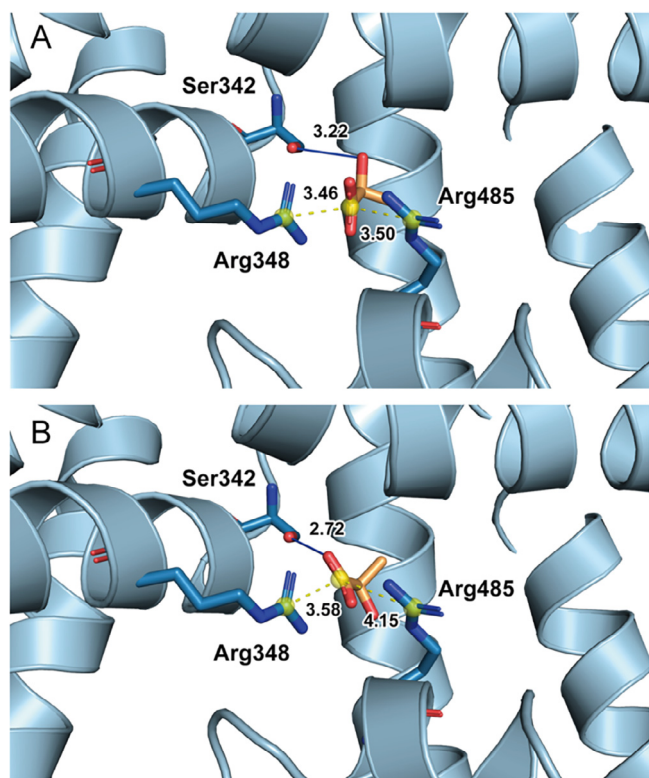


Fig. 5. Molecular docking results of HSA–L-Lac and HSA–D-Lac complexes. Interaction of (A) L-Lac and (B) D-Lac with HSA (Arg348, Arg485, Ser342), respectively.

acid enantiomers' binding site. The results showed that the residues of HSA interacted with lactic acid enantiomers at Sudlow's site I located at subdomain IIA and binding conformations are shown in Fig. 5.

Fig. 5 shows that the binding pattern of L-Lac and D-Lac are similar. The carboxyl moiety of lactic acids is electronegative, and the electronegative centres form salt bridges with residues Arg348 and Arg485, respectively. The distances are 3.46 Å (L-Lac vs. Arg348), 3.58 Å (D-Lac vs. Arg348), 3.50 Å (L-Lac vs. Arg485) and 4.15 Å (D-Lac vs. Arg485). The bindings are reinforced because of the hydrogen bonding between the hydroxyl oxygen of ligands and Ser342 of HSA. The distances are 3.22 Å (for L-Lac vs. Ser342) and 2.72 Å (for D-Lac vs. Ser342), respectively. As a theoretical inference, because of structural features of lactic acid, the hydrophobic force can be ignored. From the interaction distance, we can speculate that L-Lac binds closer to HSA than does D-Lac, which was confirmed by docking scores (Grid Score, Table S3). The docking results well explained why the binding constant (K_d) of L-Lac is larger than that of D-Lac. From the Table S3, the contributions of the electrostatic force (Grid_{es}) and van der Waals force (Grid_{vdw}), that were calculated by the Grid method, were predominant in the binding. This result is consistent with the results of thermodynamic analysis: van der Waals forces and hydrogen bonds probably play key roles in the binding reaction.

There are two ways of intake D-Lac into human physiological fluids. One is absorption from foods and the other is absorption from microorganisms in the gut (McLellan, Phillips, & Thornalley, 1992). Recently, the D-Lac level in plasma has been used as a clinical marker of increased intestinal permeability after severe injuries (Tan, Wang, Liu, Ju, & Li, 2005). D-Lac is also a potential biomarker for the diagnosis of D-lactic acidosis associated with short small bowel (Bongaerts et al., 2000) and diabetes (Christopher, Broussard, Fallin, Drost, & Peterson, 1995). Both enantiomers of lactic acid may cause metabolic acidosis, but their relative contributions are distinct due to their different origins and metabolic pathways. As a consequence, revealing the interactions between

L-Lac/D-Lac and carrier protein HSA may also have biological significance.

4. Conclusions

In this research, the enantioselective interactions between L-Lac/D-Lac and HSA were investigated using multi-spectroscopic methods and molecular modelling. The binding mechanisms of lactic acid enantiomers with HSA were investigated to obtain important information, including the binding constants, binding energy, binding sites, binding forces, and conformational changes. Fluorescence quenching of HSA by lactic acid enantiomers could be caused by forming the protein-ligand ground-state complex, and thermodynamic analysis shows evidence of the interaction force type, which agrees with the results of molecular docking. The CD, synchronous and 3D fluorescence results show that the binding of lactic acid enantiomers results in slight microenvironmental and conformational changes of HSA. These results provide useful information for understanding the delivery process of lactic acid enantiomers *in vivo*. Taking lactic acid enantiomers as an example, the chiral binding mechanisms of HSA with L-Lac/D-Lac yield potential data for understanding the interaction patterns of HSA with other chiral molecules used as food ingredients (e.g. tartaric acid enantiomers, glucose enantiomers.). The study is thus valuable for reinforcing the supervision of food nutrition and safety.

Conflicts of interest

There are no conflicts to declare.

Acknowledgement

We would like to thank Dr. Zhaohui Huo in Department of Chemistry, Guangdong University of Education for her help in checking and revising this manuscript.

Funding sources

This work was supported by National Key Research and Development Program of China (2017YFC1601700), National Natural Science Foundation of China, China (31601540, 31771939), Natural Science Foundation of Guangdong Province, China and Guangdong and Guangzhou S&T Plan (2016A030310304, S2013030013338, 2017B020207010, 2016201604030004), Provincial Key Platform and Major Research Projects of Guangdong Universities (2015KQNCX106), Doctoral Research Project of Guangdong University of Education (2014ARF02).

Appendix A. Supplementary data

Supplementary data associated with this article can be found, in the online version, at <https://doi.org/10.1016/j.foodchem.2018.07.135>.

References

- Ali, M. S., & Al-Lohedan, H. A. (2018). Spectroscopic and computational evaluation on the binding of safranal with human serum albumin: Role of inner filter effect in fluorescence spectral correction. *Spectrochimica Acta Part A Molecular & Biomolecular Spectroscopy*, 203, 434–442.
- Allen, W. J., Balius, T. E., Mukherjee, S., Brozell, S. R., Moustakas, D. T., Lang, P. T., ... Rizzo, R. C. (2015). DOCK 6: Impact of new features and current docking performance. *Journal of Computational Chemistry*, 36(15), 1132–1156.
- Alm, L. (1982). Effect of Fermentation on L(+) and D(-) lactic acid in milk. *Journal of Dairy Science*, 65(4), 515–520.
- Alonso, H., Bliznyuk, A. A., & Gready, J. E. (2006). Combining docking and molecular dynamic simulations in drug design. *Medicinal Research Reviews*, 26(5), 531–568.
- Bongaerts, G., Bakkeren, J., Severijnen, R., Sperl, W., Willems, H., Naber, T., ... Tolboom, J. (2000). Lactobacilli and acidosis in children with short small bowel. *Journal of Pediatric Gastroenterology and Nutrition*, 30(3), 288–293.
- Cao, X. Y., Wang, S., Tian, S. Q., Lou, H., Kong, Y. C., Yang, Z. J., & Liu, J. L. (2018).

- Spectroscopic and molecular modeling studies on the interactions of fluoranthene with bovine hemoglobin. *Spectrochimica Acta Part A Molecular & Biomolecular Spectroscopy*, 203, 301–307.
- Christopher, M. M., Broussard, J. D., Fallin, C. W., Drost, N. J., & Peterson, M. E. (1995). Increased serum d-lactate associated with diabetic ketoacidosis. *Metabolism*, 44(3), 287–290.
- Congdon, R. W., Muth, G. W., & Splittgerber, A. G. (1993). The binding interaction of Coomassie blue with proteins. *Analytical Biochemistry*, 213(2), 407–413.
- Duran, M., Van Biervliet, J. P. G. M., Kamerling, J. P., & Wadman, S. K. (1977). D-Lactic aciduria, an inborn error of metabolism? *Clinica Chimica Acta*, 74(3), 297–300.
- Flemström, G. (1971). Intracellular accumulation and permeability effects of some weak acids in the isolated frog gastric mucosa. *Acta Physiologica Scandinavica*, 82(1), 1–16.
- Ghosh, K., Rathi, S., & Arora, D. (2016). Fluorescence spectral studies on interaction of fluorescent probes with Bovine Serum Albumin (BSA). *Journal of Luminescence*, 175, 135–140.
- Gu, Y., Wang, Y., & Zhang, H. (2018). Study on the interactions between toxic nitroanilines and lysozyme by spectroscopic approaches and molecular modeling. *Spectrochimica Acta Part A Molecular & Biomolecular Spectroscopy*, 202, 260–268.
- He, X. M., & Carter, D. C. (1992). Atomic structure and chemistry of human serum albumin. *Nature*, 358(6383), 209–215.
- Jakalian, A., Bush, B. L., Jack, D. B., & Bayly, C. I. (2000). Fast, efficient generation of high-quality atomic charges. AM1-BCC model: I. Method. *Journal of Computational Chemistry*, 21(2), 132–146.
- Jakalian, A., Jack, D. B., & Bayly, C. I. (2002). Fast, efficient generation of high-quality atomic charges. AM1-BCC model: II. Parameterization and validation. *Journal of Computational Chemistry*, 23(16), 1623–1641.
- Kelly, S. M., Jess, T. J., & Price, N. C. (2005). How to study proteins by circular dichroism. *Biochimica et Biophysica Acta (BBA) – Proteins and Proteomics*, 1751(2), 119–139.
- Lakowicz, J. R. (2013). *Principles of fluorescence spectroscopy*. New York: Springer Science & Business Media.
- Liu, Z., Liu, Y., Zeng, G., Shao, B., Chen, M., Li, Z., ... Zhong, H. (2018). Application of molecular docking for the degradation of organic pollutants in the environmental remediation: A review. *Chemosphere*, 203, 139–150.
- Matei, I., Ionescu, S., & Hillebrand, M. (2011). Interaction of fisetin with human serum albumin by fluorescence, circular dichroism spectroscopy and DFT calculations: Binding parameters and conformational changes. *Journal of Luminescence*, 131(8), 1629–1635.
- McLellan, A. C., Phillips, S. A., & Thornalley, P. J. (1992). Fluorimetric assay of d-lactate. *Analytical Biochemistry*, 206(1), 12–16.
- Mu, H., Xu, Z., Liu, Y., Sun, Y., Wang, B., Sun, X., ... Dzantiev, B. B. (2018). Probing the stereoselective interaction of ofloxacin enantiomers with corresponding monoclonal antibodies by multiple spectrometry. *Spectrochimica Acta Part A Molecular & Biomolecular Spectroscopy*, 194, 83–91.
- Mukherjee, S., Balias, T. E., & Rizzo, R. C. (2010). Docking validation resources: Protein family and ligand flexibility experiments. *Journal of Chemical Information and Modeling*, 50(11), 1986–2000.
- Food Policy and Nutrition Div. FAO, World Health Organization, Geneva, & ESN. (1974). *Toxicological evaluation of some food additives including anticaking agents, antimicrobials, antioxidants, emulsifiers and thickening agents*. WHO Food Additives Series No. 5. XF2006131373.
- Petersen, E. F., Goddard, T. D., Huang, C. C., Couch, G. S., Greenblatt, D. M., Meng, E. C., & Ferrin, T. E. (2004). UCSF Chimera—A visualization system for exploratory research and analysis. *Journal of Computational Chemistry*, 25(13), 1605–1612.
- Ross, P. D., & Subramanian, S. (1981). Thermodynamics of protein association reactions: Forces contributing to stability. *Biochemistry*, 20(11), 3096–3102.
- Schrödinger, L. (2015). *The PyMOL molecular graphics system. version 1.8*.
- Shen, H., Gu, Z., Jian, K., & Qi, J. (2013). In vitro study on the binding of gemcitabine to bovine serum albumin. *Journal of Pharmaceutical and Biomedical Analysis*, 75(Supplement C), 86–93.
- Shiri, F., Rahimi-Nasrabadi, M., Ahmadi, F., & Ehrlich, H. (2018). Multispectroscopic and molecular modeling studies on the interaction of copper-ibuprofenate complex with bovine serum albumin (BSA). *Spectrochimica Acta Part A Molecular & Biomolecular Spectroscopy*, 203, 510–521.
- Siddiqui, G. A., Siddiqui, M. K., Khan, R. H., & Naeem, A. (2018). Probing the binding of phenolic aldehyde vanillin with bovine serum albumin: Evidence from spectroscopic and docking approach. *Spectrochimica Acta Part A Molecular & Biomolecular Spectroscopy*, 203, 40–47.
- Tan, L., Wang, Y., Liu, X., Ju, H., & Li, J. (2005). Simultaneous determination of l- and d-lactic acid in plasma by capillary electrophoresis. *Journal of Chromatography B*, 814(2), 393–398.
- Tang, B., Huang, Y., Ma, X., Liao, X., Wang, Q., Xiong, X., & Li, H. (2016). Multispectroscopic and docking studies on the binding of chlorogenic acid isomers to human serum albumin: Effects of esteryl position on affinity. *Food Chemistry*, 212, 434–442.
- Tang, L., Li, S., Bi, H., & Gao, X. (2016). Interaction of cyanidin-3-O-glucoside with three proteins. *Food Chemistry*, 196(Supplement C), 550–559.
- Wang, Y., Zhang, G., & Wang, L. (2014). Potential toxicity of phthalic acid esters plasticizer: Interaction of dimethyl phthalate with trypsin in vitro. *Journal of Agricultural and Food Chemistry*, 63(1), 75–84.
- Yuan, T., Weljie, A. M., & Vogel, H. J. (1998). Tryptophan fluorescence quenching by methionine and selenomethionine residues of calmodulin: Orientation of peptide and protein binding. *Biochemistry*, 37(9), 3187–3195.
- Zhang, G., Wang, L., & Pan, J. (2012). Probing the binding of the flavonoid diosmetin to human serum albumin by multispectroscopic techniques. *Journal of Agricultural and Food Chemistry*, 60(10), 2721–2729.
- Zhang, J., Zhuang, S., Tong, C., & Liu, W. (2013). Probing the molecular interaction of triazole fungicides with human serum albumin by multispectroscopic techniques and molecular modeling. *Journal of Agricultural and Food Chemistry*, 61(30), 7203–7211.
- Zhang, Q., & Ni, Y. (2017). Comparative studies on the interaction of nitrofurantoin antibiotics with bovine serum albumin. *Rsc Advances*, 7(63), 39833–39841.